Odd-Parity Pairing and Topological Superconductivity in a Strongly Spin-Orbit Coupled Semiconductor

Satoshi Sasaki,[1] Zhi Ren,[1] A. A. Taskin,[1] Kouji Segawa,[1] Liang Fu,[2,*] and Yoichi Ando[1,†]

[1]*Institute of Scientific and Industrial Research, Osaka University, Ibaraki, Osaka 567-0047, Japan*

[2]*Department of Physics, Massachusetts Institute of Technology, Cambridge, Massachusetts 02139, USA*

(Received 23 July 2012; published 21 November 2012)

The existence of topological superconductors preserving time-reversal symmetry was recently predicted, and they are expected to provide a solid-state realization of itinerant massless Majorana fermions and a route to topological quantum computation. Their first likely example, $Cu_xBi_2Se_3$, was discovered last year, but the search for new materials has so far been hindered by the lack of a guiding principle. Here, we report point-contact spectroscopy experiments suggesting that the low-carrier-density superconductor $Sn_{1-x}In_xTe$ is accompanied by surface Andreev bound states which, with the help of theoretical analysis, would give evidence for odd-parity pairing and topological superconductivity. The present and previous finding of possible topological superconductivity in $Sn_{1-x}In_xTe$ and $Cu_xBi_2Se_3$ suggests that odd-parity pairing favored by strong spin-orbit coupling is likely to be a common underlying mechanism for materializing topological superconductivity.

DOI: 10.1103/PhysRevLett.109.217004 PACS numbers: 74.45.+c, 03.65.Vf, 73.20.At, 74.20.Rp

Topological superconductors (TSCs) have become a research frontier in the study of topologically ordered electronic states of matter [1–4]. As a superconducting (SC) cousin of topological insulators [5,6], a TSC supports gapless surface quasiparticle states consisting of massless Majorana fermions as its distinctive characteristic. Majorana fermions are peculiar in that particles are their own antiparticles [7], and they are currently attracting significant interest because of their potential for fault-tolerant topological quantum computing [8]. The p-wave superconductor Sr_2RuO_4 has been widely discussed [9] to be an example of a chiral TSC associated with spontaneous time-reversal symmetry breaking [10]. More recently, time-reversal-invariant TSCs were theorized and attracted much attention [6]. Lately, the $Cu_xBi_2Se_3$ superconductor [11] has been theoretically proposed [4] and experimentally identified [12] as the first likely example of such a TSC. However, $Cu_xBi_2Se_3$ crystals are intrinsically inhomogeneous [13] and it has been difficult to elucidate the nature of the surface Majorana fermions. Naturally, discoveries of new TSC materials are strongly called for. In this context, $Cu_xBi_2Se_3$ is peculiar in that it is a superconductor obtained by doping a topological insulator, and such materials are few and far between; consequently, the prospect of finding new TSC materials in doped topological insulators is not very bright.

Nevertheless, the discovery of possible topological superconductivity in $Cu_xBi_2Se_3$ suggested that other TSCs might also be found in low-carrier-density semiconductors whose Fermi surface is centered around time-reversal-invariant momenta [14–16]. This motivated us to look for signatures of topological superconductivity in In-doped SnTe (denoted $Sn_{1-x}In_xTe$) [17,18] whose Fermi surface depicted in Fig. 1(a) satisfies the above criteria. In this Letter, by performing point-contact spectroscopy on $Sn_{1-x}In_xTe$ single crystals, we found evidence for the existence of a surface Andreev bound state (ABS), which is a hallmark of an unconventional superconductivity [19]. Knowing that the symmetry and low-energy physics of this material [20] allows only three types of superconducting gap functions and that all possible unconventional states are topological, it is possible to conclude that $Sn_{1-x}In_xTe$ is likely to be a TSC. This discovery not only enriches the family of possible TSC materials for their detailed investigations, but also points to a common mechanism for topological superconductivity, providing a guiding principle for the search of TSCs.

It is known that In in $Sn_{1-x}In_xTe$ acts as an acceptor and suppresses the ferroelectric structural phase transition (SPT) in SnTe. Above $x \simeq 0.04$ the SPT is completely suppressed and the system becomes a robust superconductor whose T_c gradually increases with x up to $\sim$2 K at $x \simeq 0.10$ [18]. Specific-heat measurements have confirmed bulk superconductivity with possibly a strong pairing interaction for $x = 0.044$ (where $T_c = 1.0$ K) [18], but no experiment to detect the surface ABS has been carried out so far. In this Letter, we focus on samples with $x = 0.045$ to avoid complications associated with the SPT.

SnTe crystallizes in the rocksalt structure (space group $Fm\bar{3}m$) and hence possesses the O_h point-group symmetry. Our In-doped single crystals were grown by a vapor transport method. High-purity elements of Sn (99.99%), Te (99.999%), and In (99.99%) were used as starting materials. The In concentration was measured with inductively coupled plasma atomic emission spectroscopy and was confirmed to be consistent with the observed T_c [18]. The crystallographic orientation of the surface plane was confirmed by the x-ray Laue analysis to be (001).

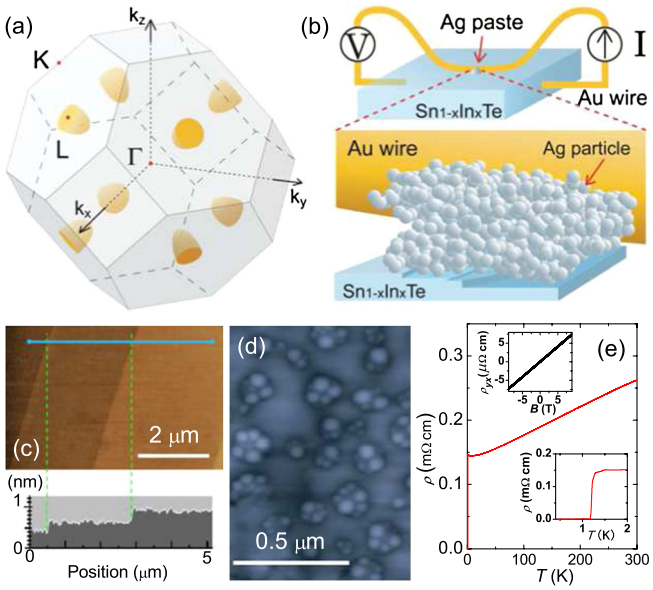

FIG. 1 (color online). SnTe and the soft point-contact spectroscopy. (a) The Fermi surfaces of p-type SnTe are centered around the four equivalent L points, which belong to the time-reversal-invariant momenta, in the bulk Brillouin zone of the cubic NaCl structure with fcc Bravais lattice. (b) Schematic picture of the soft point-contact spectroscopy experiment. (c) Atomic force microscope picture of an as-grown faceted surface of $Sn_{1-x}In_xTe$ single crystal and its height profile. (d) Atomic force microscope picture of the Ag particles on the measured surface after the gold wire is removed. (e) Temperature dependence of the resistivity of the measured sample ($x = 0.045$), showing no sign of structural phase transition. Lower inset shows a magnified view near the SC transition at 1.2 K. Upper inset shows the magnetic-field dependence of the Hall resistivity ρ_{yx} showing completely B-linear behavior, which indicates that the second valence band maxima, even if slightly populated, plays little role in our sample; the slope gives the carrier density of 8×10^{20} cm^{-3}.

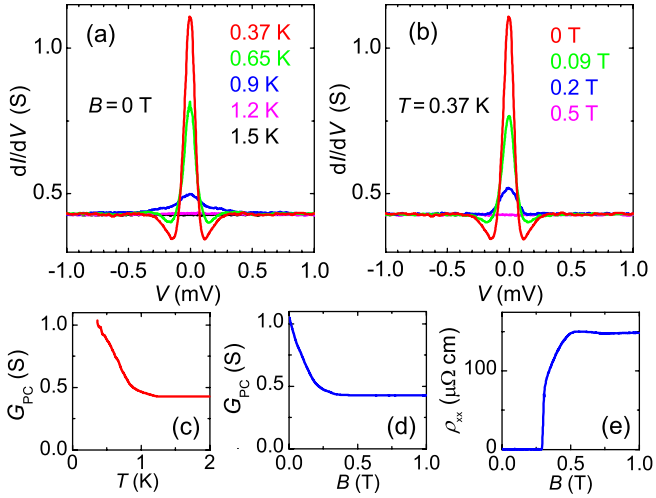

FIG. 2 (color online). Conductance spectra of $Sn_{1-x}In_xTe$. (a) Bias-voltage (V) dependence of the differential conductance, $[dI/dV](V)$, at various temperatures in 0 T. (b) $[dI/dV](V)$ in various magnetic fields at 0.37 K. (c) Temperature dependence of the zero-bias conductance in 0 T, showing its enhancement of more than a factor of 2 in the SC state at low temperature. (d) Magnetic-field (B) dependence of the zero-bias conductance at 0.37 K. (e) B dependence of the resistivity ρ_{xx} at 0.37 K showing that 0.5 T is enough to completely suppress superconductivity.

The resistivity and the Hall resistivity were measured in the Hall-bar geometry with a six-probe method on the same crystal [Fig. 1(e)]. The Quantum Design Physical Properties Measurement System was used as a platform to cool the samples down to 0.37 K and apply magnetic fields up to 9 T. The upper critical field H_{c2} defined by a sharp resistivity onset was 0.3 T at 0.37 K [Fig. 2(e)].

We performed conductance spectroscopy on the faceted (001) as-grown surface [Fig. 1(c)] of $Sn_{1-x}In_xTe$ single crystals with $x = 0.045$ [$T_c = 1.2$ K, see Fig. 1(e)] using a soft point-contact technique [21] [Fig. 1(b)] which was successfully applied to $Cu_xBi_2Se_3$ [12] to reveal its possible TSC nature. The soft point contacts were prepared by putting a tiny drop of silver paste below a 30-μm-diameter gold wire [Fig. 1(b)]; an atomic force microscope image of the silver nanoparticles on a measured surface is shown in Fig. 1(d). The dI/dV spectra were measured with a lock-in technique by sweeping a dc current that is superimposed with a small amplitude [1.8 μA (rms), corresponding to 0.7 A/cm^2] ac current, and a quasi-four-probe configuration was employed to read the voltage between a normal metal (silver paste) and the sample (see Ref. [12] for details). We show in the Supplemental Material [22] that this technique yields ordinary Andreev reflection spectra [23] when applied to the conventional s-wave superconductor Sn.

When applied to $Sn_{1-x}In_xTe$, this technique allowed us to observe an intriguing signature of ABS [24] [Figs. 2(a) and 2(b)] rather than the ordinary Andreev reflection; namely, the bias-voltage dependence of the differential conductance dI/dV presents a pronounced peak at zero voltage (i.e., Fermi level) accompanied by dips on its sides at the energy scale of the SC gap ($\pm$ 0.1 meV). In the case of the ordinary Andreev reflection [23], as one can see in Fig. S1 of the Supplemental Material [22], two peaks, rather than dips, should be observed at the SC gap energy at low enough temperatures. Moreover, in our data for $Sn_{1-x}In_xTe$, the point-contact conductance at zero energy, G_{PC}, in the SC state becomes more than twice the normal-state value [Figs. 2(c) and 2(d)], which is impossible for Andreev reflections [23] and points to the existence of ABS on the surface [19,24].

The large magnitude of the observed zero-bias conductance peak (ZBCP) is already a strong indication that it is due to an ABS, but it is prudent to examine the possible relevance of other origins of the ZBCP, such as heating effect [25], reflectionless tunneling [26], and magnetic Kondo scattering [27]. In this respect, the magnetic-field dependence of the spectra [Fig. 2(b)] gives evidence

against those other possibilities (see the Supplemental Material [22] for details) and one can conclude with reasonable confidence that the observed ZBCP is caused by an inherent surface ABS. This conclusion points to an unconventional SC state in $Sn_{1-x}In_xTe$.

To identify the nature of the SC state in $Sn_{1-x}In_xTe$, we first note that the Fermi surface in the normal state consists of four ellipsoids centered at four L points of the fcc Brillouin zone. The conduction and valence bands in the vicinity of each L point are described by the $k \cdot p$ Hamiltonian [20]:

$$H(\mathbf{k}) = m\sigma_z + v\sigma_x(k_1 s_2 - k_2 s_1) + v_3 k_3 \sigma_y. \quad (1)$$

Here k_3 is the momentum along the threefold axis ΓL; k_2 is along the twofold axis LK. s_i and σ_i are Pauli matrices associated with spin and orbital degrees of freedom, respectively. Specifically, the two orbitals labeled by $\sigma_z = \pm 1$ are mainly derived from the p orbitals of Sn and Te atoms, respectively. We emphasize that at L points these two types of p orbitals have opposite parity and do not mix. The four-band Hamiltonian (1) of $Sn_{1-x}In_xTe$ at the L points of the fcc lattice is essentially equivalent to that of $Cu_xBi_2Se_3$ at the Γ point of the rhombohedral lattice [14], both of which are dictated by the underlying D_{3d} point group symmetry.

We now discuss the possible pairing symmetries. Since the four L points are invariant under the inversion of crystal momentum $\mathbf{k} \rightarrow -\mathbf{k}$, superconducting order parameters with zero total momentum correspond to pairing *within* each Fermi pocket, and therefore consist of four components on the four Fermi pockets: $\vec{\Delta} = (\Delta_1, \Delta_2, \Delta_3, \Delta_4)$. Each Δ_j can be classified by the representations of D_{3d}, a subgroup of the O_h point group for In-doped SnTe that leaves L_j invariant. For the Hamiltonian (1) at a given L_j, there are four types of momentum-independent gap functions Δ_j with different internal spin and orbital structures, corresponding to the A_{1g}, A_{1u}, A_{2u}, and E_u representations of D_{3d} [4]. Furthermore, depending on the relative phases between $\Delta_1, \ldots, \Delta_4$, $\vec{\Delta}$ belong to different representations of the O_h point group. It is beyond the scope of this Letter to exhaust all possibilities. Instead, we consider those superconducting states that do not spontaneously break any lattice symmetry, in accordance with all experimental facts known so far. There are three such states corresponding to the following one-dimensional representations of O_h point group: A_{1g}, A_{1u}, and A_{2u}. [The E_u state breaks the threefold rotation symmetry around (111) axis.]

Among these three states, A_{1g} is even parity and fully gapped, which corresponds to an s-wave superconductor and does not have a surface ABS. Both A_{1u} and A_{2u} states are unconventional superconductors with odd-parity pairing. The A_{1u} state is fully gapped and realizes an odd-parity TSC. The topological invariant is given by $N = \sum_j N_j$, where $|N_j| = 1$ is the invariant associated with each Fermi surface and its sign is given by $\mathrm{sgn}(\Delta_j)$ [15]. Importantly, the four components $\Delta_1, \ldots, \Delta_4$ are related by rotation symmetry and have the same sign in the A_{1u} state. As a result, the A_{1u} state of In-doped SnTe is a TSC with $|N| = 4$, which supports topologically protected surface ABS.

The odd-parity A_{2u} state has point nodes at the intersection of each Fermi pocket with the ΓL line. These nodes are protected by the mirror symmetry of the fcc crystal structure. While it is impossible to define a 3D topological invariant for a gapless phase, one can still define "weak" topological invariants associated with 2D time-reversal-invariant planes in the Brillouin zone [28,29] that are fully gapped. For the A_{2u} state in In-doped SnTe, any plane that passes a *single* L point and avoids the nodes satisfies the criterion for 2D odd-parity TSC [4,30] and has a nonzero weak topological invariant. As a result, the A_{2u} state has topologically protected ABS, similar to those in the A_{2u} state of $Cu_xBi_2Se_3$ theoretically demonstrated earlier [12].

From the above analysis, we conclude that the two odd-parity states A_{1u} and A_{2u} are topologically nontrivial and support ABS that can naturally give rise to the observed ZBCP. We further propose an electron-phonon mechanism for odd-parity pairing in $Sn_{1-x}In_xTe$. First, we note that SnTe has a soft TO phonon at $\mathbf{q} = \mathbf{0}$, which couples strongly to *interband* electronic excitations [31]. This phonon mode corresponds to the displacement of Sn and Te sublattices relative to each other. It becomes unstable and leads to the SPT at low temperature. The SPT temperature is suppressed by In doping [18]. As one can see in Fig. 1(e), the temperature dependence of the resistivity shows no kink down to T_c, which indicates that the SPT is completely suppressed in our sample; according to the phase diagram [18], this is reasonable for $x = 0.045$. This suggests that the TO phonon remains stable. Moreover, proximity to the SPT suggests that the tendency toward ferroelectricity is strong, which naturally points to an attractive interaction between Sn and Te p orbitals.

Assuming that such an *interorbital* attraction from electron-phonon coupling is the origin for superconductivity, we can now theoretically deduce the pairing symmetry of $Sn_{1-x}In_xTe$ by following a similar analysis as was done for $Cu_xBi_2Se_3$ [4]. Essentially, the spin-orbit coupled band structure (1) cooperates with the above attractive interaction to favor the pairing between Sn and Te orbitals. Because the two orbitals have opposite parity, as mentioned earlier, one may conclude that the pairing symmetry in $Sn_{1-x}In_xTe$ is most likely odd parity. A detailed theory of the pairing mechanism and a full determination of the type of odd-parity pairing is beyond the scope of this Letter and will be presented elsewhere [32]. In any case, since the even-parity state does not produce a surface ABS but both odd-parity states in $Sn_{1-x}In_xTe$ do, our experimental observation strongly suggests that the odd-parity pairing is realized in this material, which agrees with the above theoretical consideration for the pairing mechanism. Given that the two possible odd-parity states are both topological

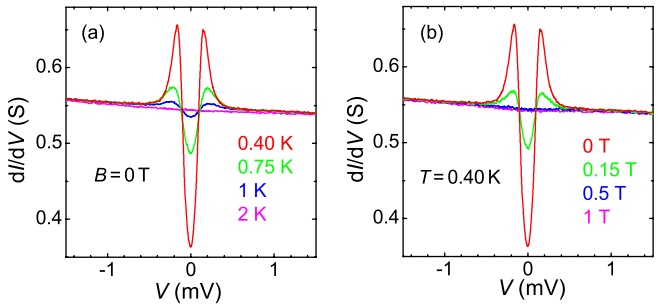

FIG. 3 (color online). Conductance spectra of $Pb_{1-x}Tl_xTe$. (a) Bias-voltage (V) dependence of the differential conductance, $[dI/dV](V)$, at various temperatures in 0 T. (b) $[dI/dV](V)$ in various magnetic fields at 0.40 K. The sample ($x = 0.013$) measured here had zero-resistivity T_c of 1.35 K and carrier density of 1.3×10^{20} cm^{-3}.

as already discussed, the present observation leads to the conclusion that $Sn_{1-x}In_xTe$ is likely to be a TSC. Note that the similarities in both band structure and pairing symmetry between $Cu_xBi_2Se_3$ and $Sn_{1-x}In_xTe$ naturally suggest that the calculations of the surface ABS performed for $Cu_xBi_2Se_3$ [12,14,33,34] should also hold qualitatively for $Sn_{1-x}In_xTe$. This means that the observed ZBCP is exactly what is theoretically expected for this type of TSC. In passing, it is useful to note that, in the conductance spectra of previously known candidate TSCs (Sr_2RuO_4 [35] and $Cu_xBi_2Se_3$ [12]), the unusual dip at the SC gap energy scale has been consistently observed, bearing strong similarly to the present spectra.

Finally, we have also studied a similar superconducting material $Pb_{1-x}Tl_xTe$ with the same point-contact technique [36]. Both $Sn_{1-x}In_xTe$ and $Pb_{1-x}Tl_xTe$ superconduct at 1–2 K [37], crystallize in rocksalt structure, and have similar band structures. Nevertheless, we found no evidence for a TSC state in $Pb_{1-x}Tl_xTe$ (Fig. 3); the observed data are consistent with the Andreev reflection spectra of conventional SC state with a low contact transparency (close to the tunneling limit). The occurrence of the conventional SC state here is probably because the pairing interaction in $Pb_{1-x}Tl_xTe$ is dominated by the charge Kondo mechanism [37] which leads to ordinary s-wave pairing. This comparison seems to indicate the importance of the TO phonon for TSC in this class of materials.

The discovery of possible topological superconductivity in $Sn_{1-x}In_xTe$ reported here is instructive for further explorations of new TSCs: It gives us a guiding principle to look for semiconductors with strong spin-orbit coupling and having Fermi surfaces surrounding time-reversal-invariant momenta, because the likely occurrence of TSC in both $Cu_xBi_2Se_3$ and $Sn_{1-x}In_xTe$ strongly suggests a common mechanism. In addition, this discovery has practical importance: While the previously discovered candidate material $Cu_xBi_2Se_3$ suffers a problem of intrinsic inhomogeneity [13] which hindered detailed studies, high-quality single crystals of $Sn_{1-x}In_xTe$ with 100% SC volume fraction are readily available. Hence, $Sn_{1-x}In_xTe$ would make it possible to explore the new topological state of matter, the time-reversal-invariant TSC, on a robust platform for the first time.

We thank T. Ueyama and R. Yoshida for technical assistance. This work was supported by JSPS (NEXT Program and KAKENHI 24740237), MEXT (Innovative Area "Topological Quantum Phenomena" KAKENHI), and AFOSR (AOARD 124038).

*liangfu@mit.edu
†y_ando@sanken.osaka-u.ac.jp

[1] A. P. Schnyder, S. Ryu, A. Furusaki, and A. W. W. Ludwig, Phys. Rev. B **78**, 195125 (2008).
[2] M. M. Salomaa and G. E. Volovik, Phys. Rev. B **37**, 9298 (1988).
[3] X.-L. Qi, T. L. Hughes, S. Raghu, and S.-C. Zhang, Phys. Rev. Lett. **102**, 187001 (2009).
[4] L. Fu and E. Berg, Phys. Rev. Lett. **105**, 097001 (2010).
[5] M. Z. Hasan and C. L. Kane, Rev. Mod. Phys. **82**, 3045 (2010).
[6] X.-L. Qi and S.-C. Zhang, Rev. Mod. Phys. **83**, 1057 (2011).
[7] F. Wilczek, Nat. Phys. **5**, 614 (2009).
[8] J. Alicea, Rep. Prog. Phys. **75**, 076501 (2012); C. W. J. Beenakker, arXiv:1112.1950.
[9] Y. Maeno, S. Kittaka, T. Nomura, S. Yonezawa, and K. Ishida, J. Phys. Soc. Jpn. **81**, 011009 (2012).
[10] N. Read and D. Green, Phys. Rev. B **61**, 10267 (2000).
[11] Y. S. Hor, A. J. Williams, J. G. Checkelsky, P. Roushan, J. Seo, Q. Xu, H. W. Zandbergen, A. Yazdani, N. P. Ong, and R. J. Cava, Phys. Rev. Lett. **104**, 057001 (2010).
[12] S. Sasaki, M. Kriener, K. Segawa, K. Yada, Y. Tanaka, M. Sato, and Y. Ando, Phys. Rev. Lett. **107**, 217001 (2011).
[13] M. Kriener, K. Segawa, Z. Ren, S. Sasaki, S. Wada, S. Kuwabata, and Y. Ando, Phys. Rev. B **84**, 054513 (2011).
[14] T. H. Hsieh and L. Fu, Phys. Rev. Lett. **108**, 107005 (2012).
[15] Y. Qi and L. Fu, APS March Meeting, http://meetings.aps.org/Meeting/MAR12/Event/168229.
[16] K. Michaeli and L. Fu, Phys. Rev. Lett. **109**, 187003 (2012).
[17] G. S. Bushmarina, I. A. Drabkin, V. V. Kompaniets, R. V. Parfen'ev, D. V. Shamshur, and M. A. Shakhov, Sov. Phys. Solid State **28**, 612 (1986).
[18] A. S. Erickson, J.-H. Chu, M. F. Toney, T. H. Geballe, and I. R. Fisher, Phys. Rev. B **79**, 024520 (2009).
[19] S. Kashiwaya and Y. Tanaka, Rep. Prog. Phys. **63**, 1641 (2000).
[20] T. H. Hsieh, H. Lin, J. Liu, W. Duan, A. Bansil, and L. Fu, Nat. Commun. **3**, 982 (2012).
[21] D. Daghero and R. S. Gonnelli, Supercond. Sci. Technol. **23**, 043001 (2010).
[22] See Supplemental Material at http://link.aps.org/supplemental/10.1103/PhysRevLett.109.217004 for supplemental data and discussions.
[23] G. E. Blonder, M. Tinkham, and T. M. Klapwijk, Phys. Rev. B **25**, 4515 (1982).

[24] Y. Tanaka and S. Kashiwaya, Phys. Rev. Lett. **74**, 3451 (1995).
[25] G. Sheet, S. Mukhopadhyay, and P. Raychaudhuri, Phys. Rev. B **69**, 134507 (2004).
[26] C. W. J. Beenakker, Phys. Rev. B **46**, 12841(R) (1992).
[27] L. Y. L. Shen and J. M. Rowell, Phys. Rev. **165**, 566 (1968).
[28] J. E. Moore and L. Balents, Phys. Rev. B **75**, 121306 (2007).
[29] L. Fu, C. L. Kane, and E. J. Mele, Phys. Rev. Lett. **98**, 106803 (2007).
[30] M. Sato, Phys. Rev. B **81**, 220504(R) (2010).
[31] S. Sugai, K. Murase, S. Katayama, S. Takaoka, S. Nishi, and H. Kawamura, Solid State Commun. **24**, 407 (1977).
[32] L. Fu *et al.* (to be published).
[33] A. Yamakage, K. Yada, M. Sato, and Y. Tanaka, Phys. Rev. B **85**, 180509(R) (2012).
[34] L. Hao and T. K. Lee, Phys. Rev. B **83**, 134516 (2011).
[35] S. Kashiwaya, H. Kashiwaya, H. Kambara, T. Furuta, H. Yaguchi, Y. Tanaka, and Y. Maeno, Phys. Rev. Lett. **107**, 077003 (2011).
[36] $Pb_{1-x}Tl_xTe$ single crystals were grown by a vapor transport method using high-purity elements of Pb (99.998%), Te (99.999%), and Tl (99.999%). The Tl concentration was measured with inductively coupled plasma atomic emission spectroscopy and was consistent with the T_c value [37]. For the point-contact experiments, $Pb_{1-x}Tl_xTe$ crystals were cleaved at room temperature in air to obtain a good (001) surface.
[37] Y. Matsushita, H. Bluhm, T. H. Geballe, and I. R. Fisher, Phys. Rev. Lett. **94**, 157002 (2005).